Factors Affecting the Accurate Prediction of Iron Losses in Electrical Machines

Conference Paper · June 2005

DOI: 10.1109/IEMDC.2005.195937 · Source: IEEE Xplore

6 authors, including:

Dan M. Ionel
University of Kentucky

Mircea Popescu
Motor Design Ltd. U.K.

Robert Heideman
A.O. Smith Corporation

Factors Affecting the Accurate Prediction of Core Losses in Electrical Machines

D. M. Ionel, M. Popescu*, S. J. Dellinger**, TJE Miller*, R. J. Heideman and M. I. McGilp*
A.O. Smith Corp., Corporate Technology Center, Milwaukee, WI 53224–9512
* SPEED Laboratory, University of Glasgow, Glasgow G12 8LT, UK
** A.O. Smith Corp., Electrical Products Company, Tipp City, OH 45371–1899

***Abstract*— A model of core losses, in which the hysteresis coefficients are variable with the frequency and induction (flux density) and the eddy-current and excess loss coefficients are variable only with the induction, is proposed. A procedure for identifying the model coefficients from multi-frequency Epstein tests is described and examples are provided for three typical grades of non grain-oriented laminated steel suitable for electric motor manufacturing. Over a wide range of frequencies between 20Hz and 400Hz and inductions from 0.05T up to 2T the new model yielded much lower errors for the specific core losses than conventional models. The applicability of the model for electric machine analysis is also discussed and examples from an interior permanent and an induction motor are included.**

Keywords — core loss, iron loss, Epstein test, laminated steel, electric machine, brushless PM motor, induction motor, finite element analysis.

I. Introduction

Since its first formulation by Steinmetz, more than a hundred years ago [1], the model of power losses in ferromagnetic materials has been continuously under study. Jordan brought a significant contribution by defining the hysteresis and eddy current components [2], on which the analysis of electrical machines is still based. Improved models based on these concepts, e.g. [3], [4], combined with careful calibration against experimental data, collected from generic motor designs, have been typically used in industrial practice.

More recently, Bertotti proposed a frequency domain model including one supplementary term of excess or anomalous loss [5]. The model, which employs material-dependent constant coefficients, was further extended into the time domain [6], gained popularity in the electrical machines community and was used in various forms in example studies, such as [7], [8] and [9]. However, the general applicability of the model remained under scrutiny and a new benchmark study, conducted by a large number of research groups in Japan, provided good correlation between a surface permanent magnet brushless motor experimental data and computations, performed with steel models that ignored the anomalous loss component [10]. In another recent paper, Boglietti et al. [11], investigated eight different materials at inductions between 0.6T and 1.7T and frequencies between 10Hz and 150 Hz, systematically identified a zero value for the excess loss coefficient and made the observation that based on Epstein frame experiments the individual contributions of eddy current and anomalous losses can not be separated. In yet another relevant paper, Chen and Pillay proposed a model with invariable coefficients for the eddy-current and excess loss and variable hysteresis loss parameters [12], an approach which combined and extended the concepts introduced by Bertotti [5], Slemon and Liu [13] and Miller et al. [3], [14].

This paper brings further original contributions to the subject by studying three different laminated steels for electric motors on a wide range of frequencies between 20Hz and 400Hz and inductions from 0.05T up to 2T. A mathematical model fitting procedure, which results in the coefficients of the core loss components being variable with frequency and/or induction, is introduced and proved to yield relatively small errors between the numerical estimations and the Epstein measurements. The comparison between the improved model and a conventional model provides interesting insights into the separation of core loss components. Also included are two example studies from a prototype interior permanent magnet (IPM) machine and an induction motor.

TABLE I
Main Characteristics of Sample Materials

Material type	Thickness	Permeability at 1.5T and 60Hz	Loss @ 1.5T at 1.5T and 60Hz	Density
	[in]	[–]	[W/lb]	[kg/m^3]
SPA	0.020	2137	2.29	7800
SPB	0.022	3071	3.16	7850
M43	0.018	1387	1.88	7700

II. Epstein Frame Measurements

One of the materials considered in the study is a widely available generic M43 fully processed electric steel. The other two materials are varieties of semi-processed cold rolled electric steel, which after annealing have the main characteristics listed in Table I and will be denoted in the following as SPA and SPB. All three steel alloys are non grain-oriented and are suitable for the high volume production of rotating electrical machines.

Samples of the materials were tested in an Epstein frame, built according to the ASTM standard [15]. The excitation and measurement system was provided by a Brockhaus Messtech-

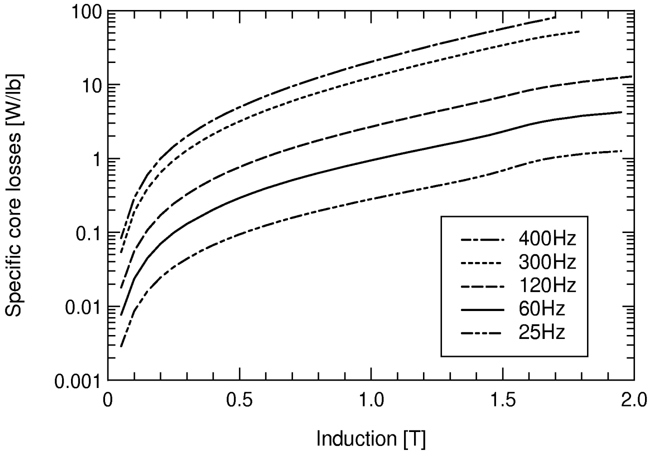

Fig. 1. Core losses measured in an Epstein frame on a sample of SPA (semi-processed electric steel of type A).

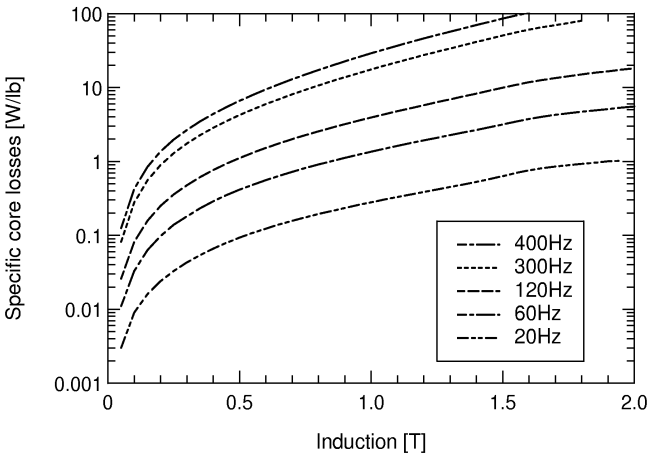

Fig. 2. Core losses measured in an Epstein frame on a sample of SPB (semi-processed electric steel of type B).

nik MPG100D 3Hz–1kHz AC/DC hysteresisgraph, equipped with an amplifier rated at peak values of 40A and 110V. The repeatability of the hysteresisgraph is certified by the instrument manufacturer at 0.1% for magnetic field measurements and 0.2% for power loss measurements. Magnetic permeability and core loss measurements (Figs.1–3) were performed over a wide range of frequencies in induction increments of 0.05T, according to an experimental procedure suggested in [16]. (The terminology of core loss, rather than iron loss, and induction, rather than flux-density, follows the relevant ASTM standards [15]).

III. New Model of Specific Core Losses

Under sinusoidal alternating excitation, typical for form-factor controlled Epstein frame measurements, the specific core losses w_{Fe} in W/lb (or W/kg), can be expressed by the equation

$$w_{Fe} = k_h f B^{\alpha} + k_e f^2 B^2 + k_a f^{1.5} B^{1.5} \quad , \tag{1}$$

where the first right-hand term stands for the hysteresis loss component, the second for the eddy-current loss component and the last for the excess or anomalous loss component [5]. In a conventional model, the values of the coefficients k_h, α, k_e and k_a are assumed to be constants, invariable with frequency f and induction B.

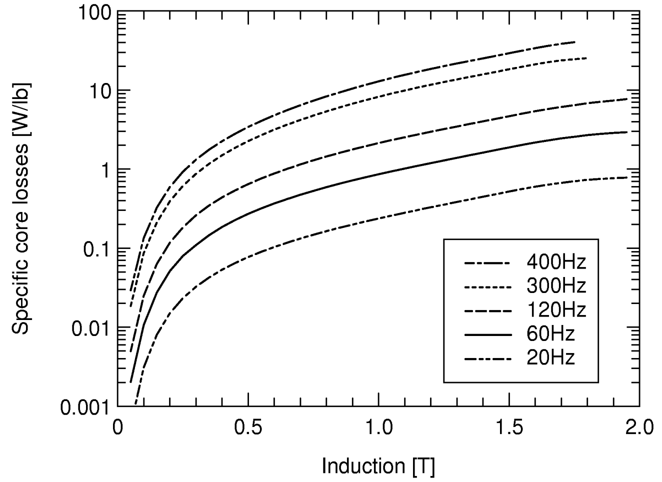

Fig. 3. Core losses measured in an Epstein frame on a sample of M43 fully processed electric steel.

As a first step of the procedure developed in order to identify the values of the coefficients, (1) is divided by the frequency resulting in

$$\frac{w_{Fe}}{f} = a + b\sqrt{f} + c\left(\sqrt{f}\right)^2 , \tag{2}$$

with:

$$a = k_h B^{\alpha} \ , \quad b = k_a B^{1.5} \ , \quad c = k_e B^2 \ . \tag{3}$$

For any induction B at which measurements were taken, the coefficients of the above polynomial in $\sqrt{f}$ can be calculated by quadratic fitting, based on a minimum of three points (Fig.4). During trials, it was observed that a sample of five points, represented by measurements at the same induction and different frequencies, is beneficial in improving the overall stability of the numerical procedure. In our study, measurements at one low frequency of 25Hz (or 20Hz), three intermediate frequencies of 60Hz, 120Hz and 300Hz, and one high frequency of 400Hz were used, where available (Figs.1–3), and, typically, the values of the fitting residual for (2) were very close to unity, i.e. $r^2 \approx 1$, indicating a very good approximation.

From (2) and (3) the eddy-current coefficient k_e and the excess loss coefficient k_a are readily identifiable. These coefficients are independent of frequency, but, unlike for the conventional model, they exhibit a significant variation with the induction (Figs. 5–6). Third order polynomials were employed for curve fitting of k_e and k_a:

$$k_e = k_{e0} + k_{e1}B + k_{e2}B^2 + k_{e3}B^3 \tag{4}$$

$$k_a = k_{a0} + k_{a1}B + k_{a2}B^2 + k_{a3}B^3 \ . \tag{5}$$

For k_e the best r^2 was obtained for SPB with a value of 0.98, followed by SPA at 0.87 and M43 at 0.75. For k_a, r^2

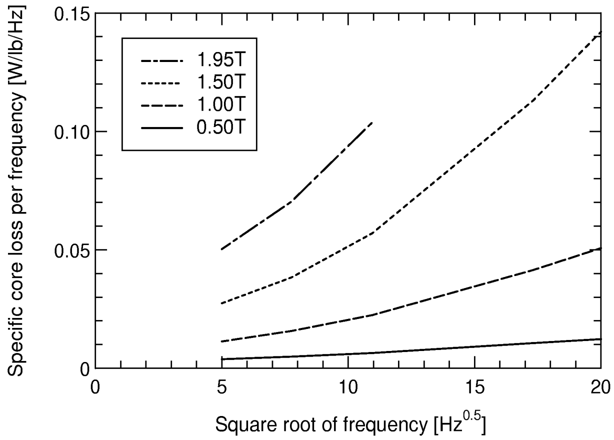

Fig. 4. The ratio of core loss and frequency w_{Fe}/f, as a function of $\sqrt{f}$ according to (2), for SPA steel.

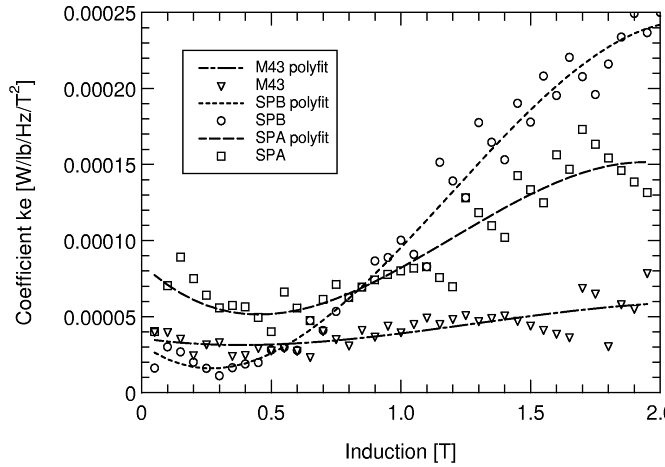

Fig. 5. The variation of the eddy-current loss component coefficient k_e with magnetic induction; k_e is invariable with frequency.

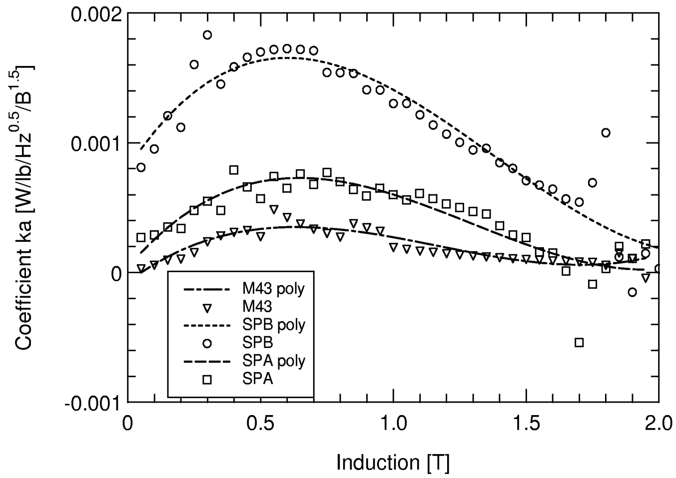

Fig. 6. The variation of the excess (anomalous) loss component k_a with magnetic induction; k_a is invariable with frequency.

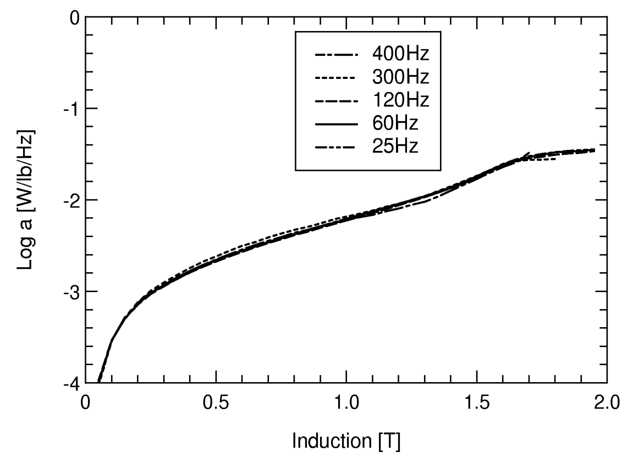

Fig. 7. The logarithm of the ratio of hysteresis loss and frequency for SPA steel; curves for different frequencies are overlapping.

varied from 0.883 for M43, to 0.82 for SPB and down to 0.78 for SPA. The discrete variations of k_e and k_a at high induction are noticeable in Figs. 5–6 and could be attributed, at least in part, to the fact that less than five fitting points were available for fitting (2).

In order to identify the coefficients k_h and α, which can be traced back to Steinmetz's original formula, further assumptions have to be made regarding their variation. An improved model, in which α is a first order polynomial of flux density, has already been in use for a number of years in a commercially available motor design software [4]. Recently, in [12] a second order polynomial has been proposed for α and in our new formulation a third order polynomial is employed

$$\alpha = \alpha_0 + \alpha_1 B + \alpha_2 B^2 + \alpha_3 B^3 \ . \tag{6}$$

Substituting (6) in (3) and applying a logarithmic operator leads to an equation

$$\log a = \log k_h + (\alpha_0 + \alpha_1 B + \alpha_2 B^2 + \alpha_3 B^3) \log B \tag{7}$$

with five unknowns, k_h and the four polynomial coefficients of α. The coefficient a represents the ratio of hysteresis loss and frequency, which is calculated from (2) by substituting the values of b and c from (3) and making use of the analytical estimators (4) and (5), which greatly reduce numerical instabilities. The plot of $\log a$ against induction at given frequency indicates three intervals of different variation type, which, for the example shown, can be approximately set to induction ranges of 0.0–0.7T, 0.7–1.4T and 1.4–2T (Fig. 7). For a given frequency and induction range, (7) is solved by linear regression using at least five induction values, i.e. $\log B$, and the discrete values of the hysteresis loss coefficients for the three materials studied are listed in Tables II-IV.

It is intesting to note that the aspect of the $\log a$ curves plotted in Fig.7 also provides support to an observation made by other authors in [10], where a two step approximation of k_h and α was proposed without the disclosure of any other details. In our model, an estimation with three induction steps is empoyed for k_h and α.

The new core loss model covers frequencies up to 400Hz and a very wide induction range between 0.05T and up to 2T and yet the relative error between the estimated and measured specific core losses is very low, as shown in Fig. 8 for SPA

TABLE II

HYSTERESIS LOSS COEFFICIENTS FOR SPA STEEL

Induction [T]	Frequency [Hz]	k_h [W/lb/T$^\alpha$]	α [–]
$B < 0.7$	25	0.0036	0.7995
	60	0.0026	0.3932
	120	0.0035	0.7839
	300	0.0028	0.3650
	400	0.0022	0.1543
$0.7 < B < 1.4$	25	0.0061	1.9085
	60	0.0061	1.9412
	120	0.0060	1.9438
	300	0.0065	1.7218
	400	0.0060	1.5924
$B > 1.4$	25	0.0329	-0.4379
	60	0.0368	-0.6895
	120	0.0349	-0.6411
	300	0.0247	-0.1990
	400	0.0210	-0.0840

TABLE III

HYSTERESIS LOSS COEFFICIENTS FOR SPB STEEL

Induction [T]	Frequency [Hz]	k_h [W/lb/T$^\alpha$]	α [–]
$B < 0.7$	20	0.0035	0.8776
	60	0.0021	0.2106
	120	0.0032	0.6674
	300	0.0015	-0.2386
	400	0.0012	-0.6309
$0.7 < B < 1.4$	20	0.0058	2.4753
	60	0.0060	2.3988
	120	0.0059	2.4502
	300	0.0056	2.5882
	400	0.0064	2.2232
$B > 1.4$	20	0.0117	1.2402
	60	0.0100	1.5328
	120	0.0063	2.5134
	300	0.0067	2.5971
	400	0.0062	2.8385

TABLE IV

HYSTERESIS LOSS COEFFICIENTS FOR M43 STEEL

Induction [T]	Frequency [Hz]	k_h [W/lb/T$^\alpha$]	α [–]
$B < 0.7$	20	0.0066	1.2184
	60	0.0053	0.9518
	120	0.0101	1.7305
	300	0.0131	2.0347
	400	0.0135	2.1005
$0.7 < B < 1.4$	20	0.0099	1.8648
	60	0.0099	1.8906
	120	0.0102	1.9086
	300	0.0110	1.9821
	400	0.0113	2.0656
$B > 1.4$	20	0.0161	1.0681
	60	0.0105	1.9251
	120	0.0110	1.8642
	300	0.0095	2.1767
	400	0.0071	2.9065

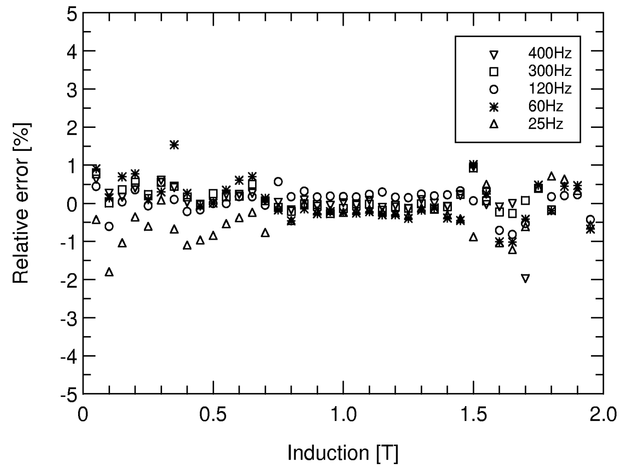

Fig. 8. The relative error between the calculated and the Epstein measured core loss at the frequencies used in the numerical model fitting for SPA steel.

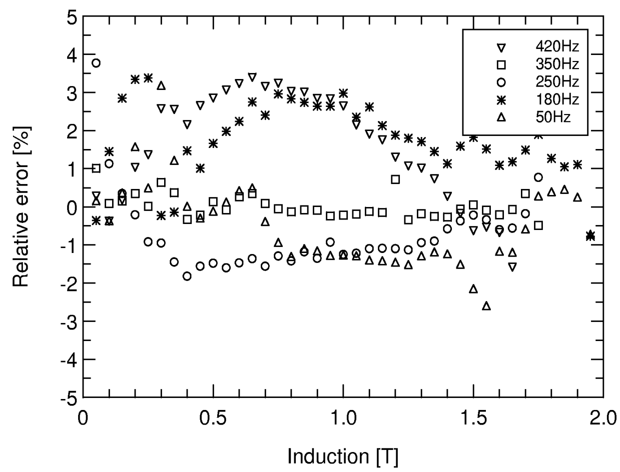

Fig. 9. The relative error between the calculated and the Epstein measured core loss at frequencies not used in the numerical model fitting for SPA steel.

steel. The errors for the SPB and M43 steel, which are not included here for brevity, are actually even lower.

The model was used to estimate losses also at frequencies not employed in the curve fitting procedure and an example is provided in Fig. 9. In this case, analytically fitted values, as per (4) and (5), were used for k_e and k_a and linearly interpolated values from Tables II-IV were employed for k_h and α. The errors are still well within limits considered satisfactory for most practical engineering applications and considerably lower than those provided by other known models, which represents, in our opinion, a remarkable result.

IV. COMPARISON WITH CONVENTIONAL MODELS

The comparison of the new model with the conventional model provides some interesting observations and, most notably, shows that the new model can be regarded as an extension of the classical theory rather than a contradiction of it. For example, conventional values for the power coefficient α from the hysteresis loss formula are typically in a range of 1.6–2.2T. In Tables II-IV with the new coefficient values, this

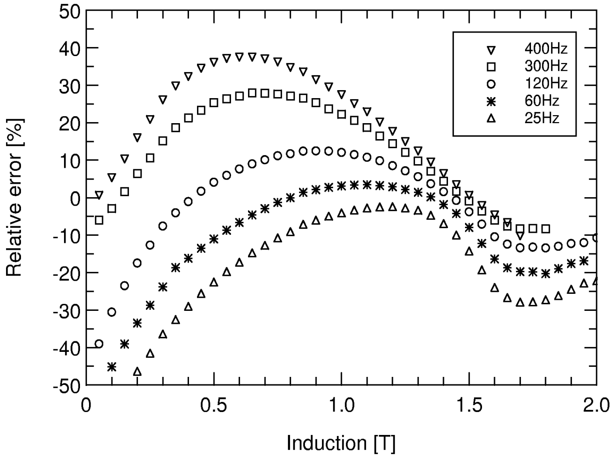

Fig. 10. The relative error between the values estimated by a conventional model with constant coefficients and Epstein measured core losses for SPA steel. The scale limits are ten times higher than in Figs. 8–9.

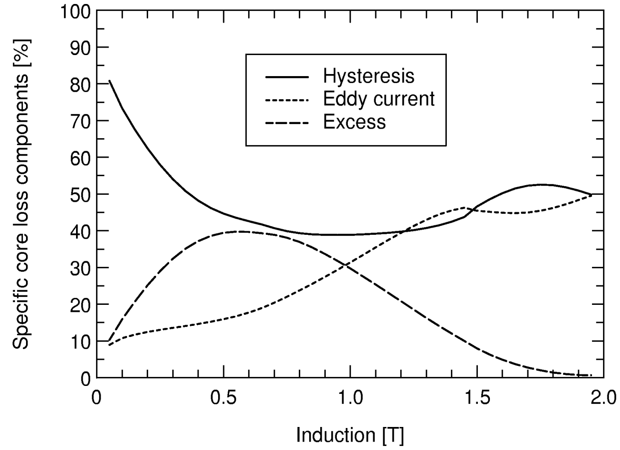

Fig. 11. Separation of core loss components at 60Hz according to the new model for SPA steel.

approximately corresponds to low frequencies and mid range inductions.

According to conventional models, the eddy current loss, which is often referred as classical loss, can be estimated with a constant value coefficient calculated as

$$k_e = \frac{\pi^2 \sigma \delta^2}{6\rho_v} \ , \tag{8}$$

based on the electrical conductivity σ, the lamination thickness δ, and the volumetric mass density ρ_V. For the materials considered, SPA, SPB and M43, the classical values of k_e correspond on the non-linear curves shown in Fig.5 at an induction of approximately 1.3T, 1.5T and 1.7T, respectively. Analytical estimations or typical values are not available for k_h and k_a.

For the purpose of a comparative exercise, coefficient values were selected to be constant and, for the hysteresis coefficients, equal to the values corresponding to 60Hz and the 0.7–1.4T range (see Table II) and, for the eddy-current and excess losses, equal to the values at 1.5T (see Figs. 5–6). The very large errors and the numerical oscillations, around the selected reference point of 1.5T, exemplified in Fig. 10, are not a surprise and are in line with previous studies published by other authors, e.g. [10].

Selecting different, but constant, values for the four coefficients may change the induction around which the errors oscillate and even reduce the maximum error, but will not be able to bring this within acceptable limits for a wide range of frequencies and inductions, due to the inherent limitations built in the conventional model. On the other hand, reliable steel models are vital, for example, for cost competitive line-fed induction motor designs, in which the magnetic loading is pushed to the very limits, and for variable speed machines, in which the flux is weakened at high speed operation and therefore accurate information of core losses at low flux density, but high frequency, is of the essence.

Oscillating errors as those illustrated in Fig. 10 also provide an interesting explanation as to why, sometimes, the calculations employing a conventional model with constant coefficients are not entirely out of proportion; provided that the flux density around which the error oscillations occur is corresponding to an "average" operating point of the magnetic circuit, overall the overestimation and the underestimation for different regions of the core will tend to cancel each other through a more or less fortunate arrangement.

While the numerical validity of the new specific core loss model is based on a systematical mathematic algorithm to identify coefficients and is proven through the small errors to measurements, its phenomenological aspects are open to debate. In particular, the separation in hysteresis, on one hand, and eddy-current and excess losses, on the other hand, is of great interest, as each of these components is receiving a different treatment in electrical machine analysis, as it will be discussed in the next section. At 60Hz and mid range inductions of 0.7–1.4T, the percentage of hysteresis out of the total core losses is relatively constant and the values calculated by the new and the conventional model are even comparable (Figs. 11–12). However, the values can be largely different at other frequencies and/or inductions (Figs. 13–14), a situation which can have direct consequences on the accuracy with which electric motors are modeled.

V. Calculation of Core Losses in Electrical Machines

The straightforward extension of a non-linear model, such as (1), from the frequency domain into the time domain, is not possible and therefore Fourier analysis, under the assumption that the contribution of the fundamental frequency is largely dominant, is the preferred engineering choice. The eddy-current and anomalous specific core losses at any point in the magnetic circuit are calculated by adding the individual contribution of each n-th harmonic:

$$w_e = \sum_{n=1}^{\infty} k_{en} (nf)^2 \left(B_{r,n}^2 + B_{t,n}^2 \right) \tag{9}$$

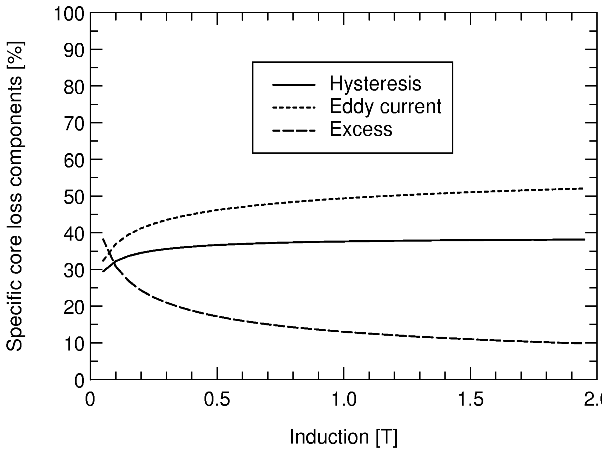

Fig. 12. Separation of core loss components at 60Hz according to a conventional model for SPA steel.

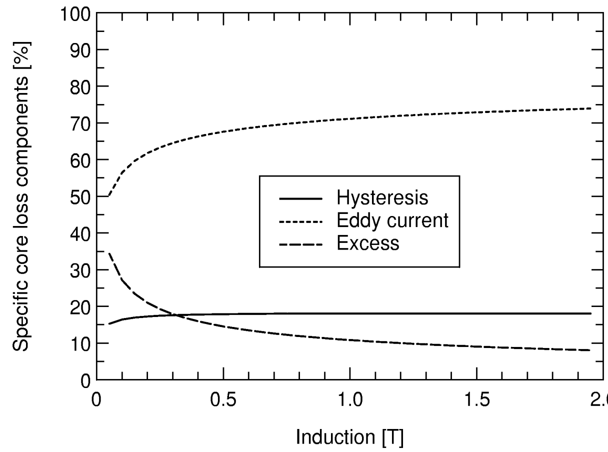

Fig. 14. Separation of core loss components at 180Hz according to a conventional model for SPA steel.

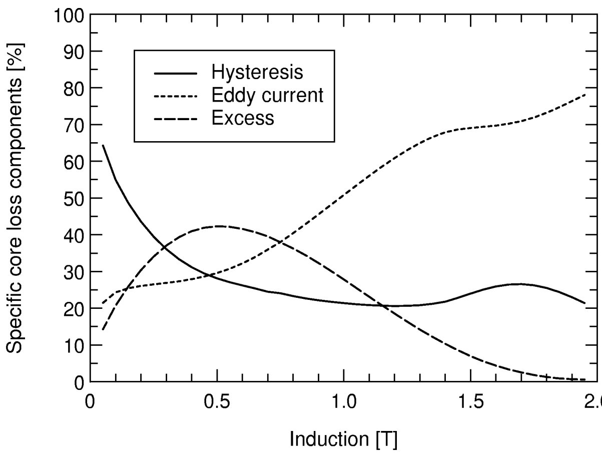

Fig. 13. Separation of core loss components at 180Hz according to the new model for SPA steel.

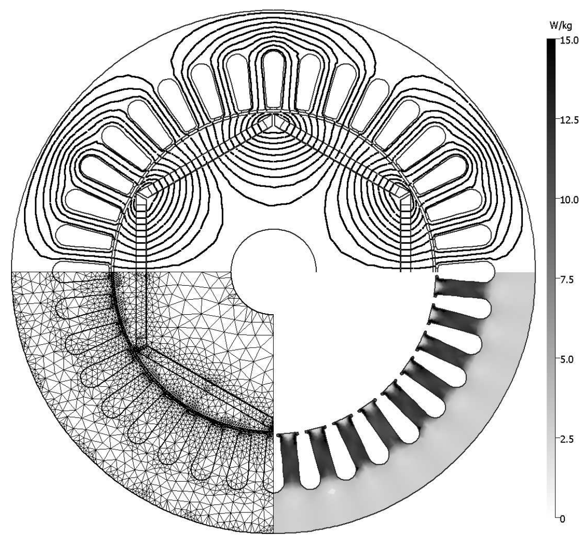

Fig. 15. Finite Element (FE) model of a 6-pole IPM machine with the distribution of specifi c core losses shown in shades of grey on a W/kg scale.

$$w_a = \sum_{n=1}^{\infty} k_{an} (nf)^{1.5} \left(B_{r,n}^{1.5} + B_{t,n}^{1.5} \right) \tag{10}$$

along the radial and tangential directions.

The hysteresis losses, on the other hand, are only dependent of the fundamental frequency f and the peak-value of the waveform of flux density B and therefore have no high harmonic contributions. The hysteresis loss is affected though by a correction factor due to the minor hysteresis loops [17].

The open-circuit core losses in the stator core of a prototype 3-phase 6-pole 184-frame prototype IPM machine with NdFeB magnets and a magnetic circuit made of SPA steel were calculated with a finite element analysis (FEA) software [18] and the previously described core loss models (Fig.15). The open-circuit operation was the preferred choice for validation in order to eliminate other unknowns, such as the exact phase current waveforms. The flux density waveforms in various parts of the stator core were decomposed in Fourier series and the harmonic contributions up to the 11-th order were added. For harmonics with a frequency exceeding 400Hz the coefficients used where those determined for 400Hz.

The comparison of computational results, obtained with the new mathematical model, for the losses in the stator core only and data from spin-down and input-output experiments (Fig. 16) is considered satisfactory, taking into account the inherent errors of such motor tests [10], the additional losses caused by the mechanical stress introduced by the frame fitting [10], and/or lamination punching, even if largely successful stress relief was provided through annealing [19]. Also the flux density in the back iron, which accounts for approximately a third of the total stator core loss, is partially exposed to rotational flux with rather significant radial and tangential components (Fig.17), which can produce rotational core losses [20]. On the other hand, the losses calculated with a conventional core loss model with constant parameters systematically overestimated the experimental data.

Similar FE computations were performed for the no-load operation of a 3-phase 2-pole 101-frame induction motor design (Fig. 18). Prototypes built from two steels, SPB and M43, were tested. In deeming as satisfactory the numerical

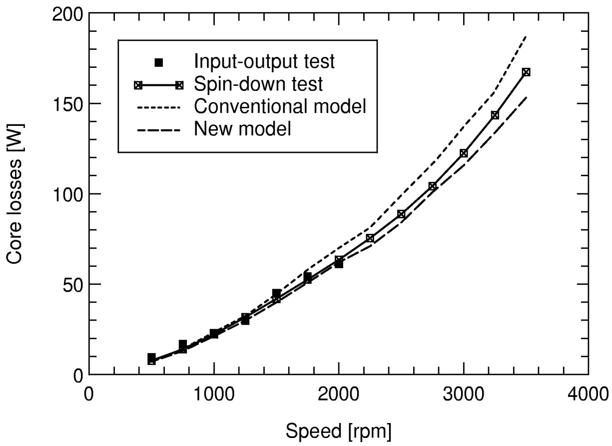

Fig. 16. Computed and measured open-circuit losses in the IPM machine.

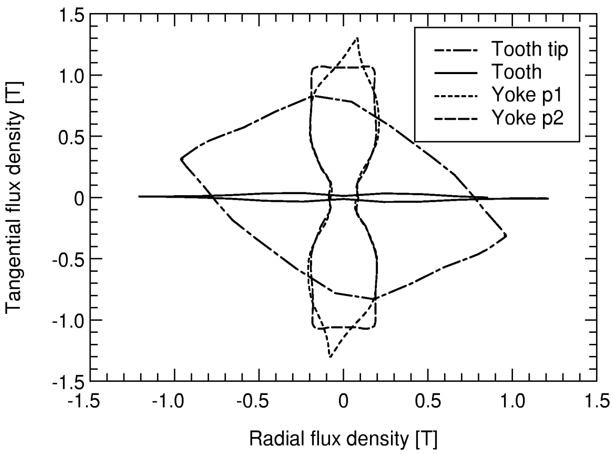

Fig. 17. Loci of magnetic flux density in the stator core of the IPM machine with two points, p_1 and p_2, exemplifed for the yoke.

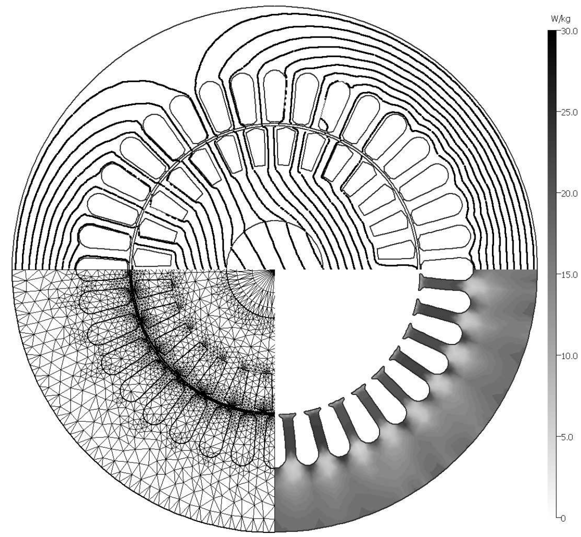

Fig. 18. FE model of a 2-pole induction motor with the distribution of specifi c core losses shown in shades of grey on a W/kg scale.

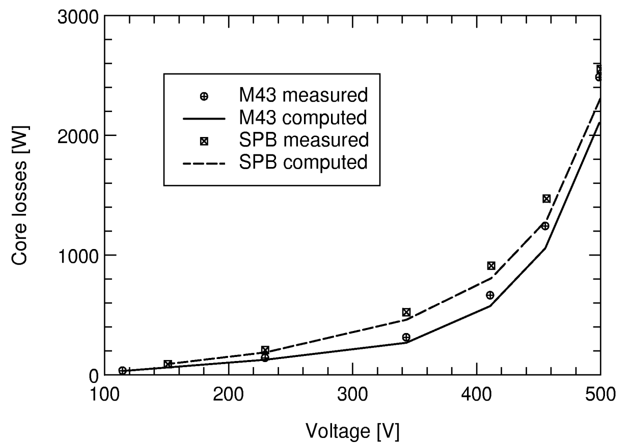

Fig. 19. Computed and measured no-load core losses in the induction motor. Protoypes were built with two different steels.

results (Fig. 19), consideration was given to possible inaccuracies due to the separation of actual stator core loss from the measurements. Also a significant fact is that the back iron, which contributes by more than 70% to the total stator core losses, is exposed to rotational magnetic flux (Fig.20), the analysis of which is beyond the scope of a model based on alternating magnetic flux data. Furthermore, the prototype design is such that at rated voltage and above, the magnetic circuit is very strongly saturated (Fig.20), this representing an extra challenge to the modeling effort.

VI. Conclusion

The proposed model uses hysteresis loss coefficients, which are variable with frequency and induction, and eddy-current and excess loss coefficients, which are variable only with the induction, and overcomes the inaccuracies of the typical conventional core loss models with constant coefficients. For the three grades of laminated electric steel studied, the errors between the computations with the new model and Epstein frame measurements are very low over a wide range of frequency between 20Hz and 400Hz and wide range of induction from as low as 0.05T and as high as 2T. A comparative study has illustrated the limitations of the conventional model and its limited applicability to 60Hz line-frequency and mid level induction in an approximate range of 0.7–1.4T.

The model with variable coefficients also provides a different perspective onto the component separation of the specific core losses, having a direct influence on electric machine analysis. While the application of the model in the daily industrial practice has to surpass the extra hurdles of collecting a substantial amount of material data, required by the numerical procedures of coefficient identification, and of FEA usage, recommended in order to obtain accurate local information on the electromagnetic field, the application of the model for research and development looks promising, especially in the light of the results obtained on two case studies from an IPM machine and an induction motor.

Acknowledgment

The authors would like to thank the colleagues at A. O. Smith Corporation, who participated in a project aimed at the

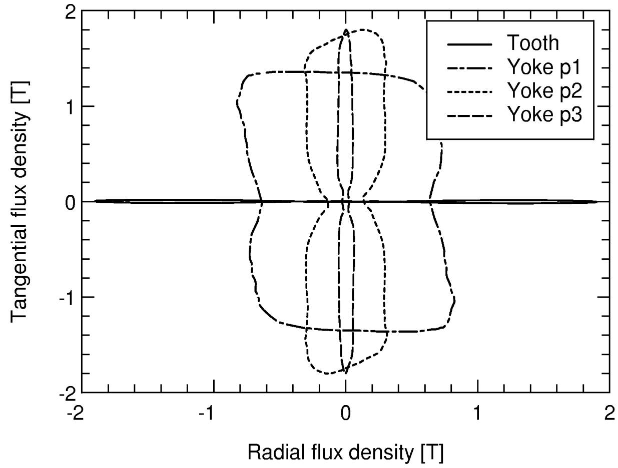

Fig. 20. Loci of magnetic flux density in the stator core of the induction motor with three points, p_1, p_2 and p_3, exemplifed for the yoke.

better characterization of electric steel, and especially to Mr. Craig Riviello and Mr. Ron Bartos.

REFERENCES

[1] C. P. Steinmetz, "On the law of hysteresis – originally published in 1892 and reprinted in," *Proc. IEEE*, vol. 72, pp. 196–221, Feb. 1984.

[2] H. Jordan, "Die ferromagnetischen konstanten fur schwache wechselfelder," *Elektr. Nach. Techn.*, 1924.

[3] J. R. Hendershot and T. J. E. Miller, *Design of Brushless Permanent-Magnet Motors*. Mentor, OH and Oxford, UK: Magna Physics and Oxford University Press, 1994.

[4] T. J. E. Miller and M. I. McGilp, *PC-BDC 6.5 for Windows – Software*, SPEED Laboratory University of Glasgow, Glasgow, UK, 2004.

[5] G. Bertotti, "General properties of power losses in soft ferromagnetic materials," *IEEE Trans. on MAG*, vol. 24, no. 1, pp. 621–630, Jan. 1988.

[6] F. Fiorillo and A. Novikov, "An improved approach to power losses in magnetic laminations under nonsinusoidal induction waveform," *IEEE Trans. on MAG*, vol. 26, no. 5, pp. 2904–2910, Sept. 1990.

[7] G. Bertotti, A. A. Boglietti, M. Chiampi, D. Chiarabaglio, and F. Fiorillo, "An improved estimation of iron loss in rotating electrical machines," *IEEE Trans. on MAG*, vol. 27, no. 6, pp. 5007–5009, Nov. 1991.

[8] K. Atallah, Z. Q. Zhu, and D. Howe, "An improved method for predicting iron losses in brushless permanent magnet dc drives," *IEEE Trans. on MAG*, vol. 28, no. 5, pp. 2997–2999, Sept. 1992.

[9] M. A. Mueller, S. Williamson, T. Flack, K. Atallah, B. Baholo, D. Howe, and P. Mellor, "Calculation of iron losses from time-stepped finite-element models of cage induction machines," in *Conf. Rec. IEE EMD'95, IEE Conf. Pub. 412*, Durham, UK, Sept. 1995, pp. 88–92.

[10] H. Domeki, Y. Ishihara, C. Kaido, Y. Kawase, S. Kitamura, T. Shimomura, N. Takahashi, T. Yamada, and K. Yamazaki, "Investigation of benchmark model for estimating iron loss in rotating machine," *IEEE Trans. on MAG*, vol. 40, no. 2, pp. 794–797, Mar. 2004.

[11] A. Boglietti, A. Cavagnino, M. Lazzari, and M. Pastorelli, "Predicting iron losses in soft magnetic materials with arbitrary voltage supply: an engineering approach," *IEEE Trans. on MAG*, vol. 2003, no. 2, pp. 981–989, Mar. 2003.

[12] Y. Chen and P. Pillay, "An improved formula for lamination core loss calculations in machines operating with high frequency and high flux density excitation," in *IEEE 37th IAS Annual Meeting Conf. Rec.*, Pittsburgh, PA, Oct. 2002, pp. 759–766.

[13] G. Slemon and X. Liu, "Core losses in permanent magnet motors," *IEEE Trans. on MAG*, vol. 26, no. 5, pp. 1653–1655, Sept. 1990.

[14] T. J. E. Miller, D. Staton, and M. I. McGilp, "High-speed pc based cad for motor drives," in *Conf. Rec. Power Elect. EPE'93*, Brighton, UK, 1993, pp. 435–439.

[15] ***, *A343/A343M–03 Standard Test Method for Alternating-Current Magnetic Properties of Materials at Power Frequencies Using Wattmeter-Ammeter-Voltmeter Method and 25-cm Epstein Test Frame*, ASTM, American Soc. for Testing and Materials, 2003.

[16] K. E. Blazek and C. Riviello, "New magnetic parameters to characterize cold-rolled motor lamination steels and predict motor performance," *IEEE Trans. on MAG*, vol. 40, no. 4, pp. 1833–1838, July 2004.

[17] J. D. Lavers, P. Biringer, and H. H. Hollitscher, "A simple method of estimating the minor loop hysteresis loss in thin laminations," *IEEE Trans. on MAG*, vol. 14, no. 5, pp. 386–388, Sept. 1978.

[18] T. J. E. Miller and M. I. McGilp, *PC-FEA 5.0 for Windows – Software*, SPEED Laboratory University of Glasgow, Glasgow, UK, 2002.

[19] A. Smith and K. Edey, "Influence of manufacturing processes on iron losses," in *Conf. Rec. IEE EMD'95, IEE Conf. Pub. 412*, Durham, UK, Sept. 1995, pp. 77–81.

[20] C. A. Hernandez-Aramburo, T. C. Green, and A. C. Smith, "Estimating rotational iron losses in an induction machine," *IEEE Trans. on MAG*, vol. 39, no. 6, pp. 3527–3533, Nov. 2003.